Proceedings of the 5th International Conference on Nanotechnology: Fundamentals and Applications
Prague, Czech Republic, August 11-13, 2014
Paper No. 136

Nanoparticle Generation from Various Seed Particles by Molecular Dynamics

Donguk Suh, Kenji Yasuoka
Keio University, Department of Mechanical Engineering
3-14-1 Hiyoshi, Kohokuku, Yokohama, Japan
suh@mech.keio.ac.jp; yasuoka@mech.keio.ac.jp

Xiao Cheng Zeng
University of Nebraska-Lincoln, Department of Chemistry
536 Hamilton Hall, Lincoln, Nebraska, USA
xzeng1@unl.edu

Abstract **–** Nanoparticle growth by vapor-liquid-solid heterogeneous nucleation was studied by classical molecular dynamics. To understand how the seed characteristics affect the condensation phenomenon, seed particles with various configurations and sizes were examined. One solid seed is placed inside a periodic cubic system with supersaturated vapor of argon molecules. The seed is a sphere, cube, rod, or tube and is made by aluminum or silicon atoms depending on the shape. Three different size classes (number of molecules forming the seed) were tested for the sphere, cube, and rod, whereas two different sizes were investigated for the tube. A broad spectrum of supersaturation ratios were simulated based on a canonical ensemble. The Yasuoka-Matsumoto method was used to calculate the growth rate around the seed. Small sizes grew faster due to the definition of the growth rate, which is correlated to the surface area. Though the number of molecules in the seed does not vary, just by changing the seed shape, the growth around the seed increases orderly for the cube compared to the sphere. Furthermore, the aspect ratio effect was investigated by elongating the cube to generate a rod, which was observed to grow slower, and the pore effect was verified for the tube. The results of this study suggest that different rates of nanoparticle growth can be achieved by simply varying the initial shape of the precursor particle.

Keywords**:** Heterogeneous nucleation, Molecular dynamics, Seed particle, Nanoparticle growth.

1. Introduction

Nanoparticle growth, which in general originates from nucleation, is important for its broad range of applications in the environment, new material generation, and medicine (Altman et al., 2004; Chen, 2008; Grass et al., 2010). To study nanoparticle growth, molecular dynamics (MD) simulation was used because it is a deterministic and microscopic method. Most of the heterogeneous nucleation studies originated from nucleation on surfaces (Kholmurodov et al., 2001; Yasuoka et al., 2000). Recently, there has been a variety of research on simulating heterogeneous nucleation with different precursor particles that act as seeds (Darvas et al., 2011; Matsubara et al., 2009; Walsh et al., 2009). Recent studies examine seed particles with basic geometric configurations such as spheres and cubes (Inci & Bowles, 2011; Suh & Yasuoka, 2011, 2012).

The current study is a review on heterogeneous nucleation occurring on precursor particles with various shapes such as a sphere, cube, rod, and tube. The objective is to understand how the physics of vapor-to-liquid phase transition on solids are affected by the change in shape and size of the seed particle, and the system supersaturation ratio (S). One solid seed is placed inside a cubic system that is filled with a monatomic gas, and the system is quenched to reproduce supersaturation.

The following section will provide a brief summary of the simulation setup, which will be ensued by the results.

Table 1. Details of dimensions of seeds placed inside system.

Seed Type	Seed Size	Characteristic Length		Surface Area (σ_{Al}^2)
Sphere	110	$5.644\sigma_{Al}$		$100\sigma_{Al}^2$
	255	$7.727\sigma_{Al}$		$188\sigma_{Al}^2$
	502	$9.563\sigma_{Al}$		$287\sigma_{Al}^2$
Cube	108	$3.651\sigma_{Al}$		$80.0\sigma_{Al}^2$
	256	$5.189\sigma_{Al}$		$162\sigma_{Al}^2$
	500	$6.732\sigma_{Al}$		$272\sigma_{Al}^2$
Rod	108	$1.59\sigma_{Al}$	$18.28\sigma_{Al}$	$121\sigma_{Al}^2$
	256	$2.40\sigma_{Al}$	$24.57\sigma_{Al}$	$248\sigma_{Al}^2$
	500	$3.12\sigma_{Al}$	$30.96\sigma_{Al}$	$406\sigma_{Al}^2$
Tube	250	$5.78\sigma_{Si}$	$18.9\sigma_{Si}$	$693\sigma_{Si}^2$
	500	$11.4\sigma_{Si}$	$18.9\sigma_{Si}$	$1353\sigma_{Si}^2$

2. Simulation Setup

The dimensions of the seeds for the sphere and cube are presented in table 1. All length dimensions are nondimensionalized by the aluminum molecular length σ_{Al}=0.255nm or σ_{Si}=0.22nm (Agrawal et al., 2002; Zimmerman et al., 2011). Details of the simulation setup can be found in the following references (Suh & Yasuoka, 2011, 2012). All particles interact via the Lennard-Jones potential, and a carrier gas was mimicked by omitting the attractive part of the potential. The target and carrier atoms both had argon properties σ_{Ar}=3.405 Å for the molecular length and 1.67×10^{-21} J (119.8 K) for the potential well depth. The seed molecules were aluminum for the sphere, cube, and rod (Agrawal et al., 2002) and silicon for the tube (Zimmerman et al., 2011). Though the molecules constructing the tube were constrained by the RATTLE algorithm (Allen & Tildesley, 1989), the molecules for the other shapes freely vibrated. There were 21,952 argon-like molecules, and among them 10,000 were carrier molecules, and the addition of the number of seed molecules in table 1 gives the total number of molecules within a system. The system volumes were scaled to the total number of particles within the system to control the initial number density of the system. The target-seed and seed-seed interactions are basically LJ interactions that use the Lorentz-Berthelot relations, and velocity rescaling was used on the carrier molecules to control the system temperature. Additionally, time integration was performed by the leap-frog Verlet algorithm, and a time step of 5.0 fs and a cutoff radius of 4.5 σ_{Al} was used throughout the entire simulation (Holcomb et al., 1992; Mecke et al., 1997; Yasuoka & Matsumoto, 1998). Nine supersaturation ratios were evaluated, and five replications were conducted for each seed type. To obtain better statistics for the nucleation and growth rates, the data from the five replications were merged into one in order to apply the Yasuoka-Matsumoto (YM) method (Yasuoka & Matsumoto, 1998). Details of the YM method and the rationale to its use are thoroughly explained in Suh and Yasuoka (Suh & Yasuoka, 2011). In addition, a Stillinger radius of 1.5 σ_{Al} (1.8 σ_{Si}) is used to define a cluster (Agrawal et al., 2002; Stillinger Jr, 1963). Figure 1 shows all seed shapes, and Fig. 2 is a snapshot of the initial system with a tube with 500 molecules as the precursor seed.

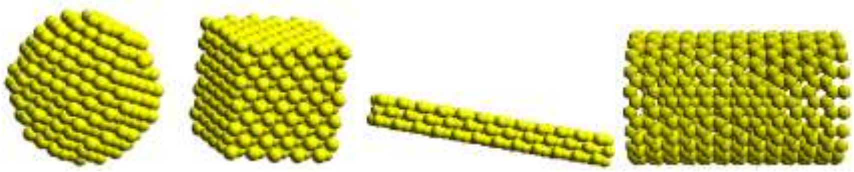

Fig. 1. Seed configurations. Sphere, cube, rod, and tube from left to right.

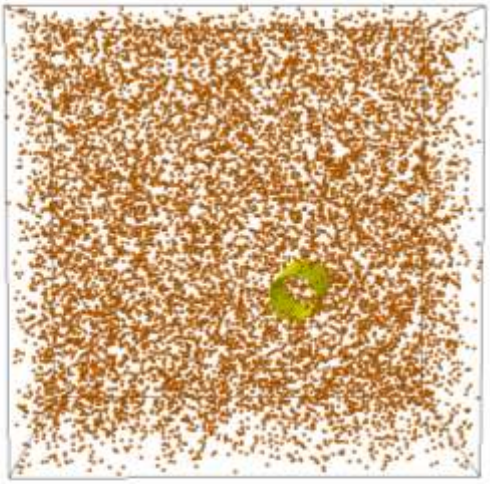

Fig. 2. Snapshot of tube with 500 molecules at 0.0 ns.

3. Results

The growth rate (J) is defined as the number of molecules that attach on the seed surface per time per surface area. The smaller the seed size as in Fig. 3(a) the faster the growth rate, where this effect can be attributed to the definition of the growth rate. Furthermore, as in Fig. 3(b), the cubic seed has an overall higher growth rate compared to the sphere, which is evidence of a shape effect. The shape effect does not show a clear seed size dependence, nor an *S* dependence. This result is consistent with the Kelvin effect, where a curved surface has a higher vapor pressure and thus the local *S* decreases for curved surfaces.

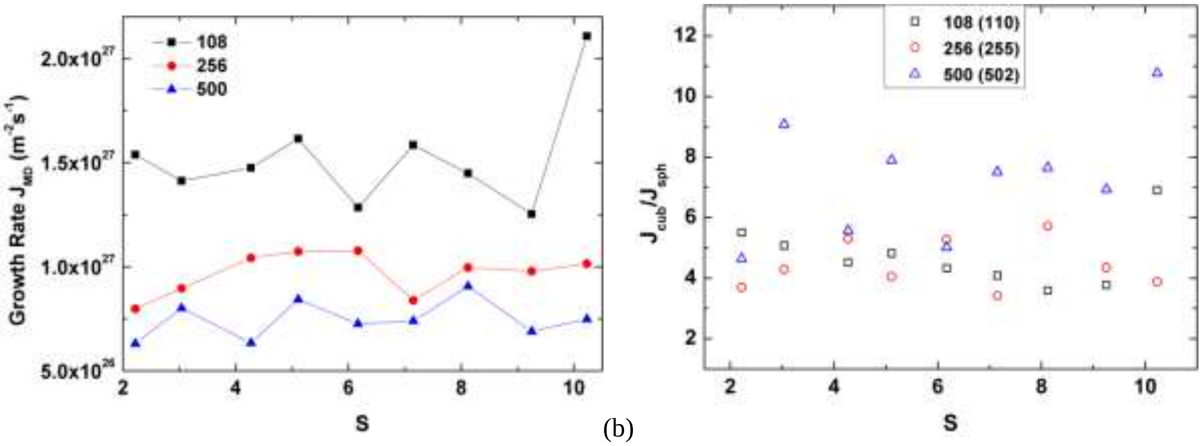

(a) (b)

Fig. 3. Plot for growth rate of (a) cubic seed and (b) comparison between cubic and spherical seed. Reprinted with permission from the Journal of Physical Chemistry B (Suh & Yasuoka, 2012). Copyright 2014 American Chemical Society.

The rod growth is also slower than the cube but faster than the sphere (figure not shown). Although the cube has an aspect ratio of 1.0, the rods here have aspect ratios around 10. However, the lower growth rate for the rod compared to the cube should be attributed more towards the difference in surface area unlike the discrepancy between the cube and sphere.

The tubes also show a lower growth rate compared to the rod (figure not shown). This can also be attributed to the surface area being double for the inner and outer surfaces of the tube. Though the tube has two surfaces for collection of vapour, it does not overcome the surface area cost in the calculation of the growth rate.

4. Conclusion

The findings of this study present the fact that the variation in the shape can induce or retard nanoparticle generation. Therefore, in the process of creating nanoparticles, being able to control the initial sizes and shapes of the precursor particles can alter the uniformity of the later sample. Furthermore, unlike homogeneous nucleation, the growth on the particles showed no supersaturation ratio dependence. This is because the nucleation mechanism and growth mechanism are dominated by thermodynamics and kinetics, respectively.

References

Agrawal, P. M., Rice, B. M., & Thompson, D. L. (2002). Predicting trends in rate parameters for self-diffusion on FCC metal surfaces. *Surface Science, 515*(1), 21-35.

Allen, M. P., & Tildesley, D. J. (1989). *Computer Simulation of Liquids*: Oxford University Press, USA

Altman, I. S., Agranovski, I. E., & Choi, M. (2004). On nanoparticle surface growth: MgO nanoparticle formation during a Mg particle combustion. *Applied Physics Letters, 84*(25), 5130-5132.

Chen, Z. (2008). Age-related differences in pulmonary and cardiovascular responses to SiO2 nanoparticle inhalation: Nanotoxicity has susceptible population. *Environmental Science & Technology, 42*(23), 8985-8992.

Darvas, M., Picaud, S., & Pal, J. (2011). Water adsorption around oxalic acid aggregates: a molecular dynamics simulation of water nucleation on organic aerosols. *Physical Chemistry Chemical Physics, 13*(44), 19830-19839.

Grass, R. N., Limbach, L. K., Athanassiou, E. K., & Stark, W. J. (2010). Exposure of aerosols and nanoparticle dispersions to in vitro cell cultures: A review on the dose relevance of size, mass, surface and concentration. *Journal of Aerosol Science, 41*(12), 1123-1142.

Holcomb, C. D., Clancy, P., Thompson, S. M., & Zollweg, J. A. (1992). A critical study of simulations of the Lennard-Jones liquid-vapor interface. *Fluid Phase Equilibria, 75*(C), 185-196.

Inci, L., & Bowles, R. K. (2011). Heterogeneous condensation of the Lennard-Jones vapor onto a nanoscale seed particle. *Journal of Chemical Physics, 134*(11).

Kholmurodov, K. T., Yasuoka, K., & Zeng, X. C. (2001). Molecular dynamics simulation of supersaturated vapor nucleation in slit pore. II. Thermostatted atomic-wall model. *Journal of Chemical Physics, 114*(21), 9578-9584.

Matsubara, H., Ebisuzaki, T., & Yasuoka, K. (2009). Microscopic insights into nucleation in a sulfuric acid-water vapor mixture based on molecular dynamics simulation. *Journal of Chemical Physics, 130*(10).

Mecke, M., Winkelmann, J., & Fischer, J. (1997). Molecular dynamics simulation of the liquid-vapor interface: The Lennard-Jones fluid. *Journal of Chemical Physics, 107*(21), 9264-9270.

Stillinger Jr, F. H. (1963). Rigorous basis of the Frenkel-Band theory of association equilibrium. *Journal of Chemical Physics, 38*(7), 1486-1494.

Suh, D., & Yasuoka, K. (2011). Nanoparticle Growth Analysis by Molecular Dynamics: Spherical Seed. *Journal of Physical Chemistry B, 115*(36), 10631-10645.

Suh, D., & Yasuoka, K. (2012). Nanoparticle Growth Analysis by Molecular Dynamics: Cubic Seed. *Journal of Physical Chemistry B, 116*(50), 14637-14649.

Walsh, M. R., Koh, C. A., Sloan, E. D., Sum, A. K., & Wu, D. T. (2009). Microsecond Simulations of Spontaneous Methane Hydrate Nucleation and Growth. *Science, 326*(5956), 1095-1098.

Yasuoka, K., Gao, G. T., & Zeng, X. C. (2000). Molecular dynamics simulation of supersaturated vapor nucleation in slit pore. *Journal of Chemical Physics, 112*(9), 4279-4285.

Yasuoka, K., & Matsumoto, M. (1998). Molecular dynamics of homogeneous nucleation in the vapor phase. I. Lennard-Jones fluid. *Journal of Chemical Physics, 109*(19), 8451-8462.

Zimmerman, P. M., Head-Gordon, M., & Bell, A. T. (2011). Selection and Validation of Charge and Lennard-Jones Parameters for QM/MM Simulations of Hydrocarbon Interactions with Zeolites. *Journal of Chemical Theory and Computation, 7*(6), 1695-1703.